Available online at www.sciencedirect.com
ScienceDirect
Journal of Power Sources 177 (2008) 553–560
JOURNAL OF POWER SOURCES
www.elsevier.com/locate/jpowsour

Studies on the degradation of Li-ion batteries by the use of microreference electrodes

J. Zhou [a,*], P.H.L. Notten [a,b]

[a] *Department of Chemical Engineering and Chemistry, Eindhoven University of Technology, 5600 MB Eindhoven, The Netherlands*
[b] *Philips Research Laboratories, High Tech Campus 4, 5656 AE Eindhoven, The Netherlands*

Received 22 August 2007; accepted 13 November 2007
Available online 21 November 2007

Abstract

Li-ion batteries made by the Lithylene technology were investigated after extensive cycling for a mechanistic understanding of the capacity fade phenomena. The batteries cycled 500 times at 0.5 C were found to lose 13% of their original capacity, which was solely due to the loss of active materials. The negative electrode maintained its capacity to contain Li^+ ions from the positive electrode. The loss of positive electrode materials was attributed to formation and thickening of the surface layer and structure disorder evidenced by XRD measurements. *In situ* impedance measurements revealed that the positive electrode was also responsible for the impedance rise upon cycling. The charge transfer resistance was found to be the most influential factor in the battery impedance, which increased exponentially during cycling. This increase was proved not due to the decrease of positive electrode surface area but resulted from growth of the surface layer.

Keywords: Li-ion batteries; Degradation; Active material loss; Impedance increase

1. Introduction

Li-ion batteries are nowadays widely used as power sources for a wide variety of electronic devices by virtue of their high cell voltage, high energy density and excellent cyclability. However, Li-ion batteries unavoidably lose some capacity irreversible upon cycling. This capacity loss is often referred to as capacity fade or degradation. Numerous researchers have studied the capacity degradation in Li-ion batteries [1–6]. In general, the possible causes for capacity fade can be classified in two categories:

i. Loss of active material: this can stem from phase changes of active material to inactive material [7], active material dissolution [8], lithium metal deposition [9], loss of contact between the active material and the current collector, and between the particles of the active material [1]. Any loss of the positive electrode material means loss of recyclable Li^+ ions. The loss of the negative electrode material results in a decreasing capacity to host Li^+ ions, which may consequently lead to lithium metal deposition.
ii. Increase of the overall battery impedance: a high battery impedance can shorten the available discharge time (and capacity) upon cycling [10].

This paper investigates the capacity fade phenomena of Li-ion batteries constructed with the proven Lithylene technology. The above-mentioned possible causes are examined. The objective herein is twofold: to identify which electrode contributes mostly to the capacity fade, and to figure out the contribution of the loss of active material and increase in battery impedance to the battery capacity loss. Lithium metal microreference electrodes [11] are used to monitor the potential profiles of the positive and negative electrodes during cycling, as well as to carry out *in situ* electrochemical impedance spectroscopy (EIS) measurements.

2. Experimental

The batteries tested in this work are based on the conventional Li-ion chemistry and were assembled with the Lithylene

* Corresponding author. Current address: Philips Research Laboratories, High Tech Campus 4 (WAG02), 5656 AE Eindhoven, The Netherlands.
Tel.: +31 40 2744010; fax: +31 40 274 3352.
E-mail address: jiang.zhou@philips.com (J. Zhou).

0378-7753/$ – see front matter © 2007 Elsevier B.V. All rights reserved.
doi:10.1016/j.jpowsour.2007.11.032

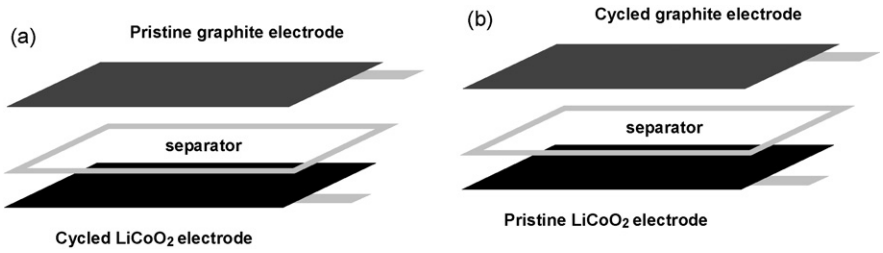

Fig. 1. Different hybrid battery configurations.

technology [12]. The positive and negative electrodes were $LiCoO_2$ and graphite, respectively (both from SKC, South Korea). The electrolyte was battery-grade LP70 (1 M LiPF6 in EC:DEC:DMC = 2:1:2, w/w) from Merck, Germany. Celgard 2300 membranes were employed as separator. All the materials were used as-received. The microreference electrodes were prepared following the recipe described elsewhere [11]. The batteries were hermetically sealed in airtight, Al-polymer bags.

The Li-ion batteries were formed before cycling with an automatic cycling apparatus (Maccor 4000 lab unit, U.S.A.), using a CCCV (constant current, constant voltage) regime. Charging was performed at 0.2 C until 4.2 V. The voltage was then kept constant until the current dropped to 0.05 C. After a resting period of 30 min, the batteries were discharged at 0.2 C until the cut-off voltage of 3 V was reached.

A similar CCCV protocol was adopted in cycle life tests. During the CC part the batteries were charged at a constant current until 4.2 V. In the CV mode the voltage was kept at 4.2 V until the cut-off current of 0.05 C was reached. Discharge was carried out galvanostatically at different C-rates with a cut-off voltage of 3.0 V. The rest time between charge and discharge was 30 min. Basically, the batteries were cycled at 0.5 C, but every 10 cycles there was one deep-discharging cycle using a current of 0.2 C. The potential plots of both the positive and negative electrodes, measured with the microreference electrodes, were recorded during cycling by means of the auxiliary inputs of the Maccor equipment.

After extensive cycling, some batteries were discharged at 0.02 C to 3.0 V twice with a rest of 3 h in-between each discharge in order to ensure that the batteries were indeed fully discharged. These fully discharged batteries were dismantled in an Ar-filled glove box. The electrodes were washed in DMC for 24 h and then dried in the glove box [3]. Each cycled positive electrode was re-assembled with a pristine negative electrode to construct a new battery, which is schematically shown in Fig. 1a. Similarly, batteries each consisting of a cycled negative electrode and a pristine positive electrode were also constructed as depicted in Fig. 1b. After being sealed in air-tight Al-polymer package and filled with electrolyte, these batteries were subjected to the capacity tests.

The electrochemical impedance spectroscopy (EIS) measurements were carried out with an Autolab PGSTAT 20 (Ecochemie, The Netherlands), using the Frequency Response Analyser (FRA) mode and under potentiostatic control. The impedance spectra were obtained by applying a sine wave of 5 mV in amplitude in the frequency range of 10 kHz–10 mHz.

The energy dispersive spectroscopy (EDS) was obtained with a Philips XL 40 FEG scanning electron microscope (SEM) attached with an EDAX Genenis 2000. The accelerating voltage was 10 kV.

The X-ray diffraction (XRD) measurements were performed with a Philips X'Pert MPD diffractometer, equipped with a Cu X-ray source and a monochromator in the diffracted beam.

Transmission electron microscopy (TEM) samples were made from both the pristine and cycled positive electrodes. Pieces of the positive electrode were ultrasonically deagglomerated in acetone. Droplets of the suspension were dispersed on an amorphous carbon film supported by a standard TEM Cu grid. The samples were analyzed by an FEI Tecnai F30ST Transmission Electron Microscope operated at 300 kV. Oxide particles were stable during the observation under the electron beams.

3. Results and discussion

3.1. Loss of active materials

Fig. 2 shows, as an example, the decrease in discharge capacity with increasing cycle number. In this case, the battery was basically cycled at 0.5 C (filled squares) while for every 10 cycles there was one cycle at 0.2 C (open triangles). Evidently, the battery attained a larger capacity at 0.2 C than at 0.5 C, which demonstrates the impact of the overall battery internal impedance on the discharge capacity.

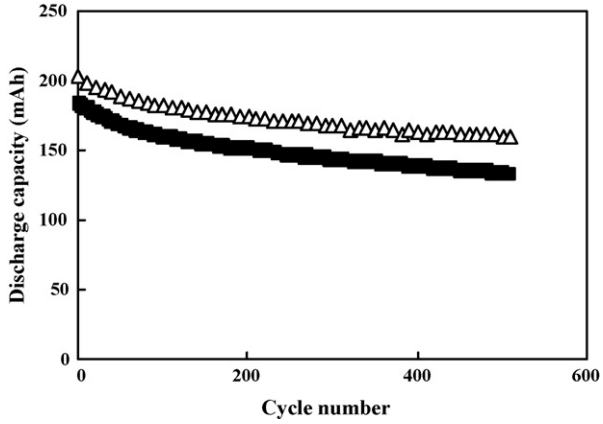

Fig. 2. Discharge capacity *vs.* cycle number. Battery had a nominal capacity of 200 mAh and was cycled at 0.5 C (■), every 10 cycles there was 1 cycle at 0.2 C (Δ).

Table 1
Discharge capacities of a 200 mAh battery at different C-rates before and after cycling

Capacity before cycling (mAh)			Capacity after cycling (mAh)		
0.02 C	0.2 C	0.5 C	0.02 C	0.2 C	0.5 C
203	200	190	176	164	132

The battery degradation can be attributed to the loss of active material and the increase in overall battery internal impedance. Fig. 2 suggests that the effect of the overall battery internal resistance on battery capacity can be minimized by using an extremely low current, thus making it possible to quantify the capacity fade solely caused by the loss of active material. In this study, a current of 0.02 C was assumed to be sufficiently low to rule out the influence of the overall battery internal resistance and therefore, the battery capacity obtained at this current was considered to be the maximum capacity of the active materials.

The discharge capacities obtained at different cycle numbers and at different discharging rates are summarized in Table 1. The maximum capacities of the battery, determined at 0.02 C before and after cycling, showed a decrease of 27 mAh. This capacity loss, accounting for 13% of its original capacity, represents the capacity fade stemming from the loss of active material.

The loss of active material can result from either the positive or negative electrode, or both of them. In Li-ion batteries, the positive electrode acts as the source of Li^+ ions while the negative electrode hosts Li^+ ions coming from the positive electrode upon charging. Obviously, the loss of positive electrode material directly leads to the loss of the battery storage capacity. The loss of the negative electrode material can result in insufficient capacity of the negative electrode to contain Li^+ ions, leading to the risk of lithium metal deposition onto the negative electrode during charging. This undesirable effect not only consumes recyclable Li^+ ions but also causes serious safety problems induced by dentrite formation.

In order to find out the capacity change of the individual electrodes upon cycling, batteries (called hybrid batteries hereafter) consisting of cycled and pristine electrodes were constructed as depicted in Fig. 1. The capacities of the hybrid batteries were determined at 0.2 C and are compared to those of the original batteries in Table 2. The capacity of the original battery dropped from 100 mAh at 1st cycle to 82 mAh after more than 500 cycles. The hybrid battery, consisting of the cycled positive electrode and a pristine negative electrode, attained a capacity of 77 mAh that was close to the 82 mAh of the original battery at the end of cycling. The capacity difference between the hybrid and the original batteries can be attributed to the consumption of Li^+ ions for the formation of the solid electrolyte interface (SEI) on the pristine graphite electrode and was observed with all the batteries examined in this work.

The battery comprising the cycled negative electrode and a pristine positive electrode gave a capacity of 100 mAh, exactly the same as the capacity the original battery exhibited at the first cycle. Obviously, the cycled negative electrode was still able to host all the Li^+ ions from the pristine positive electrode. It should be pointed out that this result does not necessarily mean that the negative electrode dose not lose any active materials at all. Many researches have shown that graphite electrode lost capacity upon cycling [13,14]. However, as the role of the negative electrode is to store Li^+ ions, the negative electrode can be considered not to contribute to the active material loss as long as it is still capable of containing all Li^+ ions coming from the positive electrode.

The results presented in Table 2 clearly reveal that the positive electrode indeed loses capacity upon cycling. Since the positive electrode provides the recyclable Li^+ ions, any process that consume recyclable Li^+ ions can lead to the loss of positive electrode material. These processes include:

i. the formation of the surface layer;
ii. lithium metal deposition on the negative electrode;
iii. dissolution of the positive electrode material;
iv. loss of contact between electrode material and current collector, loss of contact between electrode particles;
v. phase change of active material to inactive material.

In this work, these factors were examined in a qualitative way rather than in a quantitative manner.

(i) It is commonly accepted that the formation of a surface layer consumes recyclable Li^+ ions. In reality, Li^+ ions will be continuously consumed during cycling due to some unavoidable parasitic reactions such as continuing surface film formation [15,16]. As this process is inevitable during battery operation, the discussion about the loss of the positive electrode material due to the surface layer is omitted. It must be clarified that the formation and growth of the surface layer takes place on both the positive and negative electrodes. In this sense, the negative electrode is responsible for the loss of recyclable Li^+ ions as well [17].

(ii) Lithium metal deposition happens when the negative electrode is not capable of hosting all the Li^+ ions from the positive electrode. Another possible cause for lithium metal deposition is that the potential of the negative electrode decreases below the lithium metal deposition potential. In principle, the potential of a fully lithiated graphite electrode is still above 0 V *vs.* Li/Li^+, indicating that lithium metal deposition cannot take place from a thermodynamic point of view. Kinetically, however, under high-current charging conditions, the negative electrode can be polarized to such an extent that E_{neg} drops below 0 V *vs.* Li/Li^+ and lithium metal is deposited onto the surface of the electrode particles. In either cases, an E_{neg} below 0 V *vs.* Li/Li^+ is the essential condition for lithium metal deposition.

The potential profiles of E_{pos} and E_{neg} during cycling were *in situ* measured with lithium metal microreference electrodes and the results are plotted in Fig. 3. It is evidenced that E_{neg} stayed well above 0 V during cycling, indicating that lithium metal deposition did not occur under these conditions. Hence, this is not the cause for the loss of recyclable Li^+ ions for the batteries cycled at 0.5 C.

(iii) It has been noticed by some researchers [8,18] that the positive electrode material can dissolve in the electrolyte. For Li-ion batteries employing spinel $LiMn_2O_4$ as the positive

Table 2
Discharge capacities of the original 100 mAh battery and the reconstructed hybrid batteries, data obtained at 0.2 C

Capacity of the original battery (mAh)		Capacity of the hybrid battery (mAh)	
Before cycling	After 511 cycles	Cycled $LiCoO_2$ + pristine graphite	Cycled graphite + pristine $LiCoO_2$
100	82	77	100

electrode, Mn dissolution in the electrolyte appears to be a serious problem and takes great responsibility for capacity fade both on cycling and storage [18]. In contrast to $LiMn_2O_4$, $LiCoO_2$, the positive electrode used in this work, does not suffer much from active material dissolution. As reported in the literature [8], when $LiCoO_2$ electrode is cycled up to 4.3 V or above, $LiCoO_2$ dissolution becomes appreciable and cobalt can be detected on the surface of the negative electrode. In order to check this point, the negative electrodes after 510 cycles were analyzed by energy dispersive spectroscopy (EDS).

The EDS spectra of the cycled and pristine negative electrodes are presented in Fig. 4. Definitely, no cobalt was detected on the pristine and cycled negative electrode. This result verifies that $LiCoO_2$ dissolution is not an appreciable process under these cycling conditions. Checking Fig. 3 it can be found that the maximum E_{pos} was 4.26 V. This voltage is consistent with the conventional limit of reversibility of 4.3 V for $LiCoO_2$ and, according to Amatucci et al. [8], is not sufficient to dissolve $LiCoO_2$ in the electrolyte. Based on these analyses, the dissolution of $LiCoO_2$ is concluded not to contribute to the loss of positive electrode material during cycling. Aurbach et al. reported similar results on the $LiCoO_2$ electrode [4].

(iv) The electrode materials in Li-ion batteries are intercalation compounds. When the battery is operating, Li^+ ions are reversibly inserted and extracted from the electrodes. As a result, the electrode materials expand during intercalation and shrink during deintercalation. This continuous volume expansion and contraction can weaken the adhesion of the electrode material particles to the current collector and between the particles. Eventually, after long-term cycling some particles may lose contact with the current collector and other particles. These "isolated" particles cannot be utilized any more during cycling, thus leading to capacity loss [1,19].

The loss of contact between the active material and the current collector and the loss of contact between the particles of the active material sounds very possible. However, to experimentally prove this appears to be difficult. One possible method is to press the cycled electrode and afterwards re-determine the capacity of the battery. This method is based on the idea that pressing the electrode under appropriate pressure can resume the contact of the "isolated" particles with the current collector and other particles, thus regaining some capacity.

The volume change of the electrode material can also be reflected by the change of the thickness of the electrode. The thickness of a pristine single-sided positive electrode was 110 μm and increased to 120 μm (∼9%) after 500 cycles, showing a clear volume expansion. After being pressed under 4 bar, the thickness of the cycled positive electrode was reduced to its original value. The pressed positive electrode was assembled with a pristine negative electrode to fabricate a new hybrid battery. Meanwhile, a battery consisting of an un-pressed cycled positive electrode and a pristine negative electrode was also constructed. The capacities of these two batteries were determined consecutively at 0.2 C, 0.5 C, 1.5 C and 0.2 C.

The discharge capacities of the two batteries at 0.2 C and 0.5 C were equal, as evidenced by Fig. 5. When the discharge current increased to 1.5 C, the battery consisting of the pressed cycled positive electrode attained a larger capacity. As the current dropped back to 0.2 C, the two batteries

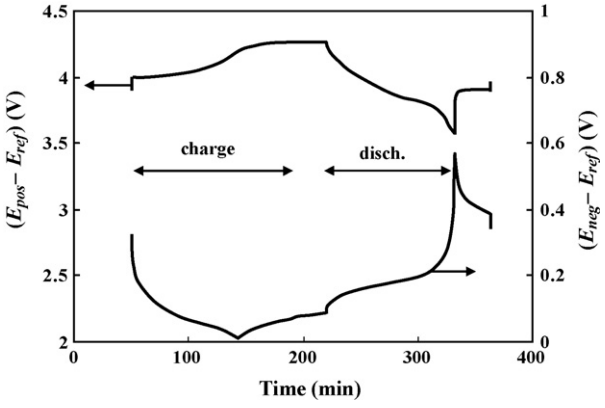

Fig. 3. Potential profiles of the positive and negative electrodes during one cycle at 0.5 C.

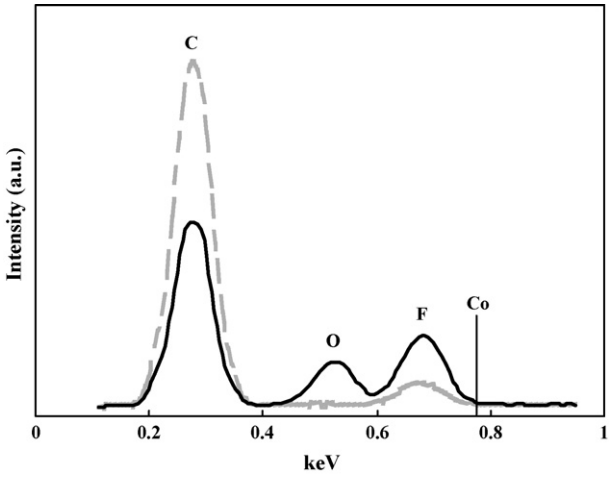

Fig. 4. EDS spectra of a pristine (dashed grey line) and a cycled (black curve) graphite electrode. The straight line marks the position of the cobalt signal.

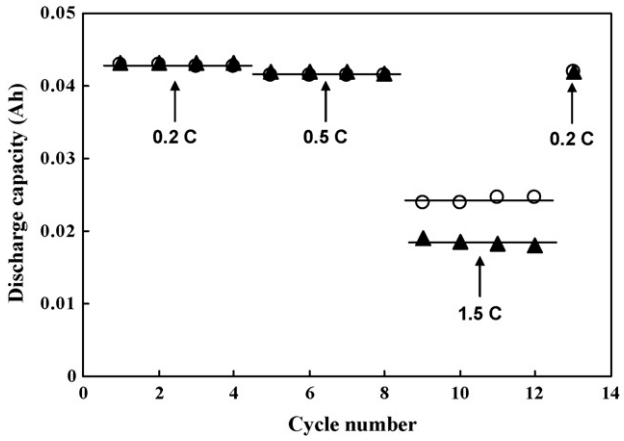

Fig. 5. Discharge capacity of two batteries at different C-rates. The batteries consisted of cycled positive electrode and pristine graphite electrode. One cycled positive electrode was pressed (◯) under 4 bar while the other was not (▲).

again delivered identical capacities. These results give a clear indication that the batteries made up of pressed and un-pressed cycled positive electrodes only had differences in internal resistance, which was reflected by the small different discharge capacities at 1.5 C. On the other hand, it appears that the capacity of the cycled positive electrode cannot be regained by pressing the electrode, as the two batteries showed identical capacity at 0.2 C. The investigation presented here may not be sufficient to prove that the cycled positive electrode does not have any "isolated" particles. Nevertheless, we tentatively conclude that the contact between the particles and the current collector and the contact between the particles for the positive electrode remained unaffected after long-term cycling and is not a plausible cause for the loss of the positive electrode.

(v) A delithiated Li_xCoO_2 ($x < 0.5$) electrode is metastable and can undergo a phase change to an electrochemically inactive structure. For a Li-ion battery in operation, the positive electrode is, most of the time, delithiated and thus very likely to experience phase transformation. Fig. 6 shows the XRD patterns of the positive electrode material before and after extensive cycling. Comparing the XRD patterns of the pristine and the cycled positive electrode, it can be noted that the characteristic peak positions of the $LiCoO_2$ phase remained unaltered, showing that no new phase had been formed. However, the relative peak intensities has substantially changed, indicating a change in the structure of the $LiCoO_2$ phase. As can be seen in Table 3, the relative intensity of the main peak (0 0 3) decreased for the cycled positive electrode. In the $LiCoO_2$ phase, alternate layers of Li and Co cations occupy the octahedral sites of a compact cubic close packing of oxide anions. A decrease in (0 0 3) peak intensity would occur when a cobalt atom occupies part of the octahedral sites of the lithium layer [20,21]. This indicates that the cation in the well-layered $LiCoO_2$ structure becomes disordered and that a portion of the Li^+ ions in the positive electrode might become inactive [5].

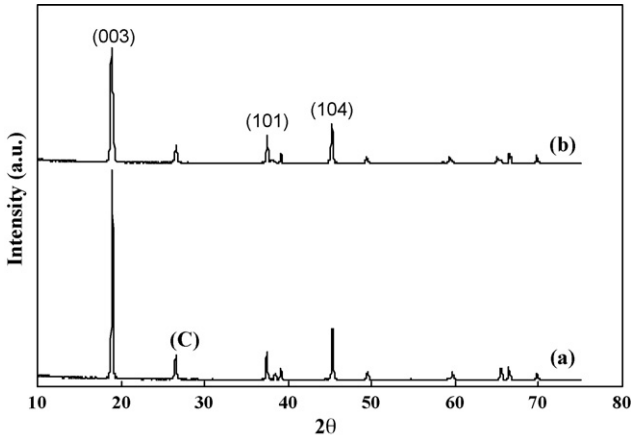

Fig. 6. XRD patterns for the positive electrode cycled at 0.5 C: (a) pristine and (b) 600 cycles.

Table 3
Change in intensity between (0 0 3) and (1 0 1) plane of a fresh and cycled positive electrode material

	Pristine electrode	Cycled electrode
Intensity of (0 0 3) peak	6555	3675
Intensity of (1 0 1) peak	900	918
I(0 0 3)/I(101)	7.3	4.0

3.2. Increase in battery impedance

One cause for battery degradation is the increase of the internal impedance upon cycling. High internal resistance shortens the time for the battery to reach the cut-off voltage during discharging, thus reducing the discharge capacity. EIS measurements reveal a remarkable increase in battery impedance upon cycling. After more than 600 cycles, the impedance was found 6 times larger.

The impedance development of the positive and negative electrodes was separately monitored during cycling. The positive electrode demonstrated a considerable increase in impedance with increasing cycle numbers as Fig. 7a shows. In contrast, the impedance of the negative electrode exhibited only little variation with respect to cycle number (see Fig. 7b). Surprisingly, the impedance of the negative electrode started to decrease after 204 cycles, which is not understood yet. By comparing the impedance spectra of the positive and negative electrodes at 608th cycle, it is indubitable that the positive electrode contributes almost solely to the increase of the total battery impedance.

In order to further reveal the properties of impedance increase, the impedance spectra of the positive electrode were fitted with an equivalent circuit (EQC) to extract the values of series resistance (R_s), resistance for Li^+ ions migrating through the surface layer (R_{SL}) and charge transfer resistance (R_{ct}) at different cycle numbers. The EQC adopted in this work is a modified Randles circuit and is used by researcher [22,23]. As expected, R_s was invariant with cycle number (Fig. 8). R_{SL} displayed a gradual increase with increasing cycle number and exhibited a tendency of leveling off after 700 cycles. The surface layer is

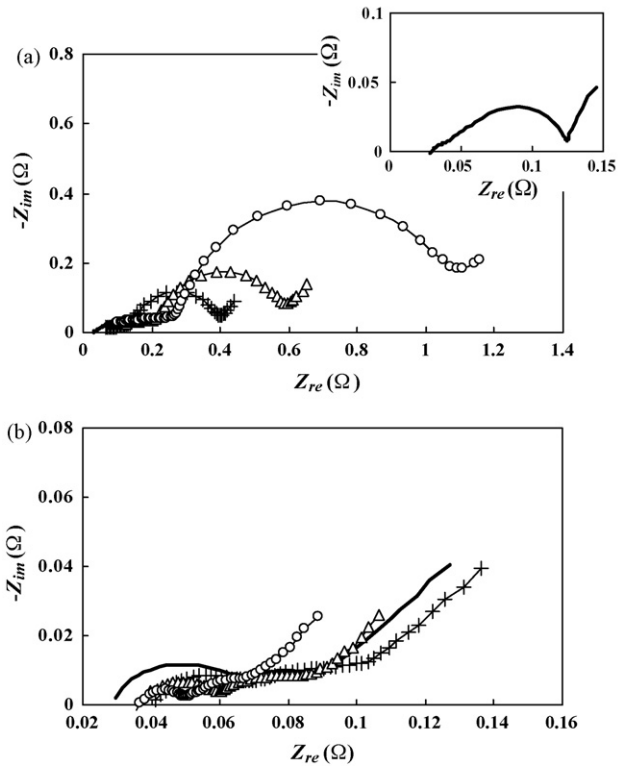

Fig. 7. Impedance spectra of (a) the positive electrode and (b) the negative electrode at 1st cycle (solid line), 204th cycle (+), 406th cycle (Δ) and 608th cycle (◯) measured with a fully charged battery. The insert enlarges the impedance spectrum of the positive electrode at the 1st cycle.

believed to continuously grow during cycling [14–16]. Thus, an increasing R_{SL}, representing the resistance for Li^+ ions to migrate through the surface layer, is physically reasonable.

The most significant factor in the impedance of the positive electrode is R_{ct}. As shown in Fig. 8, R_{ct} not only represents

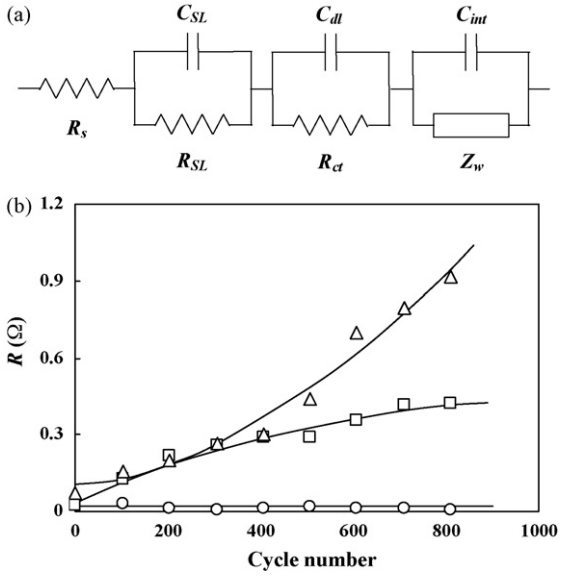

Fig. 8. (a) Equivalent circuit and (b) the development of R_s^{pos} (◯), R_{SL}^{pos} (□) and R_{ct}^{pos} (Δ) upon cycling, data extracted from the impedance spectra measured with a microreference electrode at the battery fully charged state.

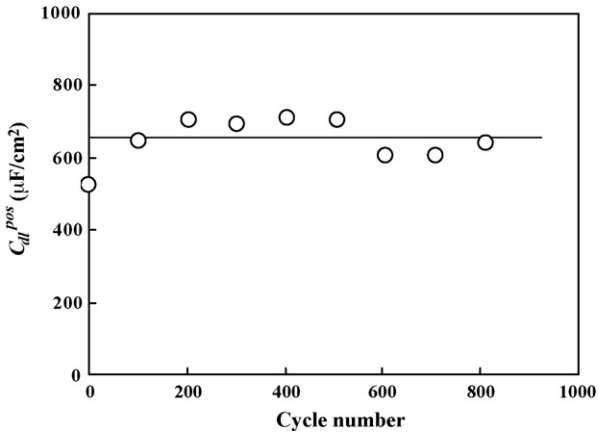

Fig. 9. Double layer capacitance *vs.* cycle number.

the largest value but also appear to increase exponentially upon cycling. The increase of R_{ct} can result from a decrease of the electrode surface area as R_{ct} is proportional to the reciprocal of surface area. The surface areas of the pristine and cycled positive electrodes were determined by Brunauer–Emmett–Teller (BET) measurements to be $2.2\,m^2\,g^{-1}$ and $2.0\,m^2\,g^{-1}$, respectively, showing that the surface area did not change after cycling. On the other hand, the double layer capacitance for the positive electrode, C_{dl} was also evaluated by fitting the impedance spectra with EQC. The obtained values of C_{dl}, which are normalized with respect to the BET surface area, are plotted in Fig. 9 and show that C_{dl} was more or less independent of cycle numbers. This result indicates that the wetted surface area indeed did not vary upon cycling because surface area is proportionally linked to C_{dl}. Both BET and C_{dl} measurements confirm that the increase in R_{ct} is not due to the change of surface area.

The origin of the R_{ct} rise upon cycling has not been clearly explained. Aurbach et al. attributed the increase in R_{ct} to the surface layer [4]. One component of the surface layer is LiF which is highly resistive to Li^+ ion migration. The increasing R_{SL} has shown that the surface layer thickens upon cycling, which makes it more difficult for Li^+ ions to migrate through this layer in order to take part in the charge transfer reaction. This, in turn, ends up with an increasing R_{ct}. Abraham et al. assigned the R_{ct} rise to the compositional change of the surface layer during cycling [24]. They argued that these compositional changes apparently increased the complexity of Li^+ ion movement through the film, resulting in an increasing resistance. Generally, the surface layer is most likely responsible for the increase in the charge transfer resistance of the positive electrode.

The particles of the positive electrode were analyzed by TEM and are shown in Fig. 10. In comparison to the pristine ones, the cycled particles were severely strained with extensive internal defects and microcracks (indicated by arrows). These defects and microcracks are believed to result from the repeated insertion and removal of Li^+ ions into and out of the positive electrode during cycling. This is partly confirmed by a comparative study on the $LiCoO_2$ particles after long-term storage. It is known that a fully charged battery loses substantial capacity after storage on a shelf. In our study, a 300 mAh Li-ion battery was found to irre-

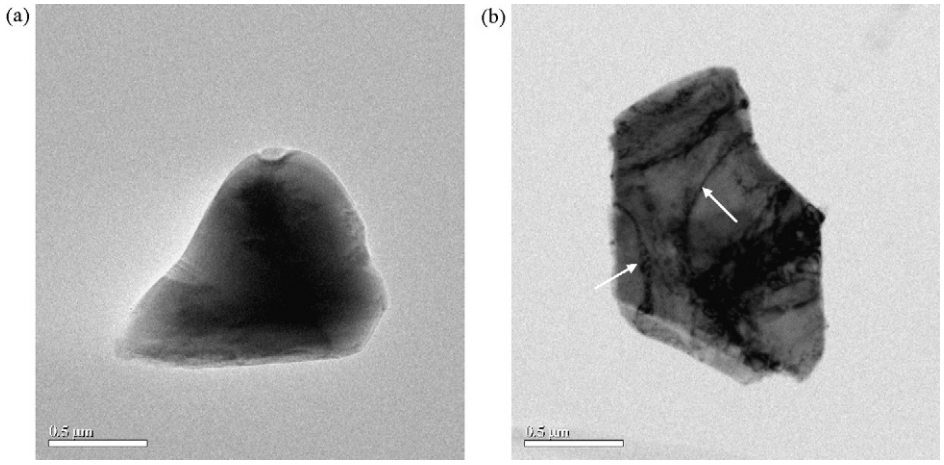

Fig. 10. TEM pictures of $LiCoO_2$ particles: (a) pristine and (b) after 500 cycles.

versibly lose a capacity of 24 mAh (8%) after 4-month storage at a fully charged state. The measured battery impedance before and after storage exhibited a similar behavior to that of the batteries after cycling (figures not shown here). The impedance of the negative electrode was almost invariant after storage whereas the positive electrode disclosed a drastic increase in impedance. The $LiCoO_2$ particles of the battery after storage were also examined by TEM. Unlike the cycled $LiCoO_2$ particles, the $LiCoO_2$ particles appeared to remain intact and no internal defects and microcracks were observed after storage. This finding indicates that the internal defects and microcracks in the cycled $LiCoO_2$ particles originate from the repeated insertion and removal of Li^+ ions. However, the role of these internal defects and microcracks in impedance rise and capacity loss during cycling is still not fully clarified.

4. Conclusions

The mechanism of capacity fade of Li-ion batteries upon cycling was investigated. It is found that the positive electrode is mainly responsible for the observed battery capacity loss. After intensive cycling, the positive electrode irreversibly lost 13% of its original capacity whereas the negative electrode maintained its capability to host all Li^+ ions.

Experimental results disclose that lithium metal deposition and dissolution of the positive electrode did not occur under the investigated conditions. The loss of contact between the electrode material and current collector and loss of contact between the electrode particles did not take place. The lost recyclable Li^+ ions are partially consumed by the surface layer. XRD measurements revealed a structure disorder, occurring in $LiCoO_2$ and a portion of the Li^+ ions in the positive electrode became inactive due to this disorder. This effect also accounts for the loss of recyclable Li^+ ions.

The battery impedance developed dramatically upon cycling. EIS measurements proved that the battery impedance rise stemmed from the positive electrode, particularly from R_{ct}. The growing surface layer may contribute to the increasing R_{ct} during cycling.

TEM studies showed that some cycled particles developed extensive internal defects and microcracks. By comparing with the $LiCoO_2$ particles after long-term storage, it is confirmed that these internal defects and microcracks result from the repeated Li^+ insertion and removal.

Finally, it is worthwhile to point out that battery capacity loss is a very complicated process. The complexity is based on the fact that many factors have an impact on degradation, which has been shown in this work. What can make battery degradation more complicated is that the causes to capacity loss vary with variant working conditions. The capacity fade rate is a function of battery working conditions that is heavily dependent on battery application. Cycling Li-ion battery at 0.5 C between 3.0 V and 4.2 V is a moderate condition. For example, lithium dissolution may occur if the batteries are charged above 4.3 V. More systematic work is required to well understand the battery degradation under various conditions.

Acknowledgements

The authors would like to thank Monique Vervest for the EDS measurements, Rene Bakker for the XRD analyses and. Dr. Jurgen van Berkum for the TEM pictures.

References

[1] P. Arora, R.E. White, M. Doyle, J. Electrochem. Soc. 145 (1998) 3647–3667.
[2] R.S. Rubino, H. Gan, E. Takeuchi, J. Electrochem. Soc. 148 (2001) A1029–A1033.
[3] J. Shim, R. Kostecki, T. Richardson, X. Song, K.A. Striebel, J. Power Sources 112 (2002) 222–230.
[4] D. Aurbach, B. Markovsky, A. Rodkin, E. Levi, Y.S. Cohen, H.-J. Kim, M. Schmidt, Electrochim. Acta 47 (2002) 4291–4306.
[5] J. Li, E. Murphy, J. Winnick, P.A. Kohl, J. Power Sources 102 (2001) 294–301.
[6] P. Ramadass, B. Haran, R. White, B.N. Popov, J. Power Sources 111 (2002) 210–220.
[7] H.F. Wang, Y.-I. Jang, B.Y. Huang, D.R. Sadoway, Y.-M. Chiang, J. Electrochem. Soc. 146 (1999) 473–480.
[8] G.G. Amatucci, J.M. Tarascon, L.C. Klein, Solid State Ionics 83 (1996) 167–173.

[9] P. Arora, M. Doyle, R.E. White, in: S. Surampudi, R. Marsh (Eds.), Lithium Batteries, The Electrochemical Society Proceedings Series, Pennington, New Jersey, 1998, p. 553.
[10] D. Aurbach, B. Markovsky, A. Rodkin, M. Cojocaru, E. Levi, H.-J. Kim, Electrochim. Acta 47 (2002) 1899–1911.
[11] J. Zhou, P.H.L. Notten, J. Electrochem. Soc. 151 (2004) A2173–A2179.
[12] P.H.L. Notten, M. Ouwerkerk, H. van Hal, D. Beelen, W. Keur, J. Zhou, H. Feil, J. Power Sources 129 (2004) 45–54.
[13] D. Zhang, B.S. Haran, A. Durairajan, R.E. White, Y. Podrazhansky, B.N. Popov, J. Power Sources 91 (2000) 122–129.
[14] G. Ning, B. Haran, B.N. Popov, J. Power Sources 117 (2003) 160–169.
[15] D. Aurbach, J. Power Sources 89 (2000) 206–218.
[16] D. Aurbach, A. Zaban, Y. Ein-Eli, I. Weissman, O. Chusid, B. Markovsky, M.D. Levi, E. Levi, A. Schechter, M. Moshkovich, E. Granot, J. Power Sources 68 (1997) 91–98.
[17] M. Broussely, S. Herreyre, P. Biensan, P. Kasztejna, K. Nechev, R.J. Staniewicz, J. Power Sources 97-98 (2001) 13–21.
[18] A. Blyr, C. Sigala, G. Amatucci, D. Guyomard, Y. Chabre, J.-M. Tarascon, J. Electrochem. Soc. 145 (1998) 194–209.
[19] A.H. Whitehead, K. Edström, N. Rao, J.R. Owen, J. Power Sources 63 (1996) 41–45.
[20] M. Yoshio, H. Tanaka, K. Tominaga, H. Noguchi, J. Power Sources 40 (1992) 347–353.
[21] E.-D. Jeong, M.-S. Won, Y.-B. Shim, J. Power Sources 70 (1998) 70–77.
[22] Y.-C. Chang, H.-J. Sohn, J. Electrochem. Soc. 147 (2000) 50–58.
[23] M. Dollé, F. Orsini, A.S. Gozdz, J.-M. Tarascon, J. Electrochem. Soc. 148 (2001) A851–A857.
[24] D.P. Abraham, E.M. Reynolds, P.L. Schultz, A.N. Jansen, D.W. Dees, J. Electrochem. Soc. 153 (2006) A1610–A1616.